Biochemical and Biophysical Research Communications 391 (2010) 806–811

Contents lists available at ScienceDirect

Biochemical and Biophysical Research Communications

journal homepage: www.elsevier.com/locate/ybbrc

Cloning and characterization of rat transient receptor potential-melastatin 4 (TRPM4)

Jae Cheal Yoo, Oleg V. Yarishkin, Eun Mi Hwang, Eunju Kim, Dong-Gyu Kim, Nammi Park, Seong-Geun Hong *,[1], Jae-Yong Park *,[1]

Department of Physiology, Institute of Health Science, and Medical Research Center for Neural Dysfunction, Biomedical Center (BK21), Gyeongsang National University College of Medicine, 90 Chilam-Dong, Jinju 660-751, South Korea

ARTICLE INFO

Article history:
Received 20 November 2009
Available online 27 November 2009

Keywords:
rTRPM4
hTRPM4
Race-PCR
Localization
Patch-clamp recording

ABSTRACT

Transient receptor potential-melastatin 4 (TRPM4) is a Ca^{2+}-activated, but Ca^{2+}-impermeable, cation channel. Increasing $[Ca^{2+}]_i$ induce current activation and reduction through TRPM4 channels. Several TRPM4 isoforms are expressed in mice and humans, but rat TRPM4 (rTRPM4) has not been previously identified. Here, we identified, cloned, and characterized two rTRPM4 isoforms, rTRPM4a and rTRPM4b, using 5′-RACE-PCR. rTRPM4b channel activity increased with $[Ca^{2+}]_i$ in a dose-dependent manner. However, the rTRPM4b Ca^{2+}-dependent activity at negative potentials differed from that of human TRPM4b (hTRPM4b), even though both represent full-length proteins. Additionally, rTRPM4b showed a slightly different single-channel current amplitude and open time distribution than hTRPM4b. However, rTRPM4a, which lacks the N-terminal region of rTRPM4b, and hTRPM4a had no similar functional channel activities. Furthermore, we characterized splicing regions, tissue distribution, and cellular localization of these isoforms. Unlike rTRPM4a, rTRPM4b was localized to the membrane at high levels, suggesting that rTRPM4b is the functionally active channel.

Introduction

The transient receptor potential (TRP) channel was originally identified in *Drosophila melanogaster* photoreceptors [1]. Three types of TRP channels have been reported in mammals: the TRP-classic (TRPC), the archetypal vanilloid receptor TRP-vanilloid (TRPV), and the TRP-melastatins (TRPMs), which are homologous to archetypal melastatin [2,3]. More than eight forms of TRPM channels have been cloned and each channel functions by a different mechanism in human [4].

TRP channels contain six transmembrane segments [5]. A hydrophobic stretch between the fifth and the sixth segments may be the cation-permeable pore. N- and C-terminal tails in the cytosolic region may engage in subunit–subunit interactions, associations with binding proteins, and interactions with cytoplasmic factors. Furthermore, TRPM4 contains putative protein kinase C and cAMP-dependent protein kinase phosphorylation sites [6].

It is known that the TRPM4b variant is a Ca^{2+}-activated and voltage-dependent Ca^{2+}-impermeable cation channel [4]. Recently, it was reported that TRPC3 as a TRPM4-binding partner negatively regulates TRPM4 channel activity [7]. Previous, we found that endogenous TRPM4 is expressed in Chinese hamster ovary (CHO) cells, making TRPM4 channel existed in the hamster [8]. In addition, the seventh amino acid of TRPM4b can attenuate deSUMOylation of the TRPM4b channel [9]. However, the function of the TRPM4 channel is poorly understood.

Several human TRPM4 (hTRPM4) isoforms have been reported, but only three isoforms have been studied in depth: (1) the full-length TRPM4 (TRPM4b), (2) an N-terminal 174 amino acid deletion isoform of TRPM4 (TRPM4a), and (3) a TRPM4 isoform lacking 537 amino acids (TRPM4c) [10]. Similarly, several isoforms of mouse TRPM4 have been characterized [10]. However, isoforms of rat TRPM4 (rTRPM4) have not been previously identified.

In this study, we identified rTRPM4a, a non-functional channel lacking the N-terminal region, and rTRPM4b, a functional channel that is an orthologue of human TRPM4b. Furthermore, we characterized rTRPM4a and TRPM4b through analysis of tissue expression, localization, and biophysical properties of the channels. Here, we find TRPM4 channels in the rat and channel property of rTRPM4.

Materials and methods

Total RNA extraction and 5′-RACE-PCR. Total RNA was extracted from rat brain using TRIzol Reagent (Invitrogen) according to the manufacturer's protocol. Concentration and purity of total RNA

* Corresponding authors. Fax: +82 55 759 0169.
E-mail addresses: hong149@gnu.ac.kr (S.-G. Hong), jaeyong@gnu.ac.kr (J.-Y. Park).
[1] These authors contributed equally to this work as co-corresponding authors.

0006-291X/$ - see front matter Crown Copyright © 2009 Published by Elsevier Inc. All rights reserved.
doi:10.1016/j.bbrc.2009.11.142

was determined by spectrophotometry on an ND-1000 spectrophotometer (Nano Drop). Using the reported rTRPM4 fragment sequence [8], full-length rTRPM4 cDNA was obtained using RACE and Reverse transcriptase-polymerase chain reaction (RT-PCR) according to the manufacturer's protocol (Full RACE Core Set, Takara). Briefly, total mRNA from rat brain was reverse transcribed. Amplified cDNA was ligated to form concatamers and circularized by T4 ligase after degradation of RNA. After combinational PCRs of the amplified cDNA, rTRPM4a and rTRPM4b were cloned.

RT-PCR analysis of rTRPM4 tissue distribution. For RT-PCR analysis, 1 μg of high-quality RNA isolated as above from several rat tissues was used. rTRPM4 was amplified using rTRPM4-specific primers (forward 5′-GAGTTGGATCCCTAAGATCTTC-3′ and reverse 5′-GGTTCTCACCACCCATGCGGCC-3′), which corresponded to the newly-identified rTRPM4 sequences. GAPDH levels were measured as an internal control.

Cell culture and transfection. This study utilized COS-7 and HEK293T cell lines. Cells were cultured in Dulbecco's modified Eagle's medium (DMEM) containing 10% fetal bovine serum (FBS), 100 units/ml penicillin, and 100 mg/ml streptomycin at 37 °C in a humidity-controller incubator with 5% CO_2. Cells were seeded at a density of 0.4×10^5 cells/ml containing five round 10-mm-diameter cover-slips. rTRPM4a and rTRPM4b were tagged with GFP on their N-terminals using the Gateway system [7]. Cells were transiently transfected with human or rat GFP-TRPM4a or GFP-TRPM4b DNA with MN-DsRed DNA using Lipofectamine™ 2000 (Invitrogen) according to the manufacturer's instructions.

Imaging analysis. Intracellular localization of human and rat TRPM4 was determined using a confocal microscope (Olympus Fluoview FV1000). For imaging analysis, cells were plated onto glass cover-slips. After co-transfection of GFP-fused genes and MN-DsRed DNA, the cells were cultured for an additional 24 h, washed twice with PBS, and then directly observed under a confocal microscope.

Patch clamp method and electrophysiology analyses. Whole-cell or single-channel recordings were performed 24 h after transfection of HEK293T cells with human or rat GFP-TRPM4a or GFP-TRPM4b. Successfully transfected cells were visually identified by their fluorescence in the patch clamp set-up.

The extracellular solution for whole-cell current measurements contained 145 mM Na-aspartate, 1 mM $MgCl_2$, 5.5 mM glucose, and 10 mM HEPES (pH 7.35). The pipette solution contained 120 mM Na-aspartate, 1 mM $MgCl_2$, 23 mM/10 mM NaOH/EGTA, and 10 mM HEPES (pH 7.20). For single-channel recordings, the pipette solution contained 145 mM Na-aspartate, 1 mM $MgCl_2$, 1.8 mM $CaCl_2$, and 10 mM HEPES (pH 7.34). The bath solution contained 145 mM Na-aspartate, 1 mM $MgCl_2$, and 10 mM HEPES (pH 7.20). $CaCl_2$ was added to EGTA-free bath solutions in a required concentration.

Whole-cell currents were recorded using a patch-clamp amplifier (Axopatch 200B, Axon Instruments, Inc.). Patch electrodes were made from borosilicate glass capillaries (World Precision Instruments, Inc.). The current–voltage relations were measured by applying ramp pulses from a holding potential of 0 mV. The ramp pulse was increased from −100 mM to 100 mM during 400 ms. The sampling interval was 200 μs and the filter setting was 5 kHz. Single-channel currents were recorded using the inside-out variant of the patch-clamp technique. Patch pipettes were made from borosilicate glass capillaries (Warner Instruments, Inc.) and coated with Sylgard (Dow Corning, USA). Single-channel currents were sampled at 5 kHz and filtered at 2 kHz using a Digidata 1200A analog–digital interface (Axon Instruments, Inc.). Experiments were performed at room temperature.

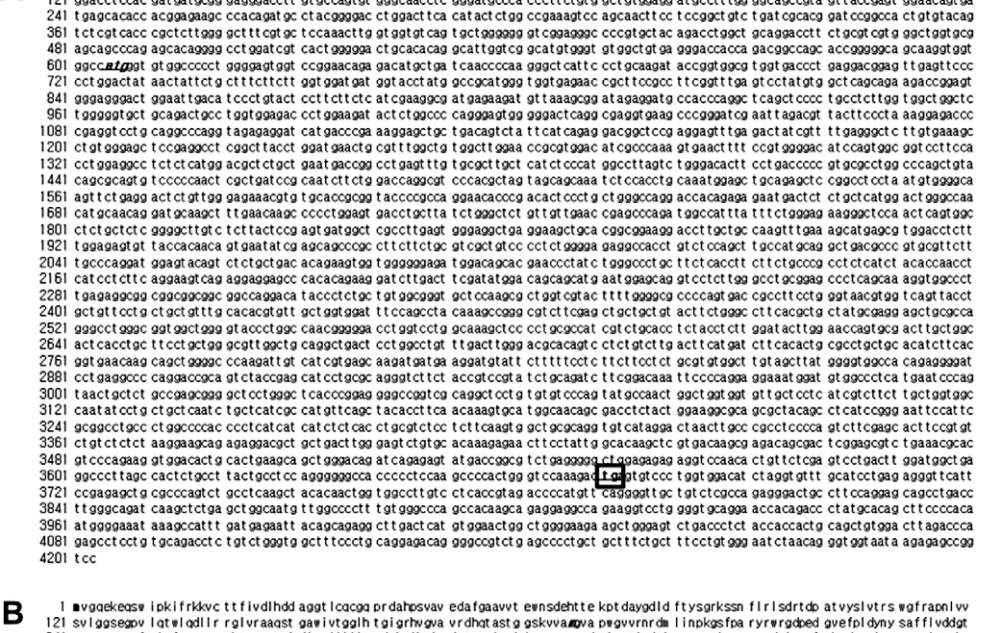

Fig. 1. Nucleotide (A) and derived amino acid sequences of the translated exons of rTRPM4 (B). The nucleotide sequences of all exons and the adjacent sequences were derived from the sequence obtained by 5′-RACE–PCR and the NCBI reference sequence (Accession No.: NP_001129701). The rTRPM4b start region is in **bold** letters (nucleotide 47) and the rTRPM4a start region is in *italic* letters (nucleotide 605). The stop codon is boxed (nucleotide 3671).

Data analysis. Currents were analyzed with Clampfit software (Axon Instruments, Inc.). Amplitude histograms were generated for the construction of I–V curves and for the estimation of channel activity (P_o). Dose–response data were fitted with a logistic function. Data are given as mean values ± SE. Significance was tested using unpaired *t* tests ($p < 0.05$).

Results

Identification of rat TRPM4 channel transcripts

Previous, we cloned about 300 bp of rTRPM4 fragment [8]. Since multiple forms of TRPM4 exist in humans and mice, we hypothesized there would be several forms in rats. Therefore, based on the rTRPM4 fragment sequence, specific primers were designed to amplify the N-and C-terminal region using RACE. Through this procedure, approximately 3000 and 3600 bp cDNA were obtained (Fig. 1A).

The predicted complete sequence of rTRPM4 was added to the NCBI Reference Sequence (Accession No.: NP_001129701). Comparison with the predicted sequence confirmed that our cDNA clone represented the full sequence of rTRPM4. To be consistent with the human nomenclature, the full-length sequence was designated rTRPM4b, and the truncated sequence was designated rTRPM4a (Fig. 1A). The complete 1208 amino acid sequence of rTRPM4b, as compared with the 1022-amino acid sequence of rTRPM4a, is presented in Fig. 1B.

Translation and expression of rTRPM4

Once the sequences were obtained for rTRPM4b and rTRPM4a, we analyzed their translation profiles. Translation of rTRPM4b started at exon I, whereas rTRPM4a translation started at exon V, since of exons III and IV are absent in TRPM4a (Fig. 2A and B). Fig. 2B shows the genomic coding sequence of the rTRPM4a and rTRPM4b start codon regions. Similar to that in humans, rTRPM4a is a 186 amino acid N-terminal deletion form of rTRPM4b.

Tissue-specific expression profiles of the newly-identified rTRPM4 isoforms were examined using comparative RT-PCR. We designed a primer set that was able to distinguish between rTRPM4a and rTRPM4b (Fig. 2A and B). rTRPM4b was expressed in various tissues, with the strongest expression in the testis, and

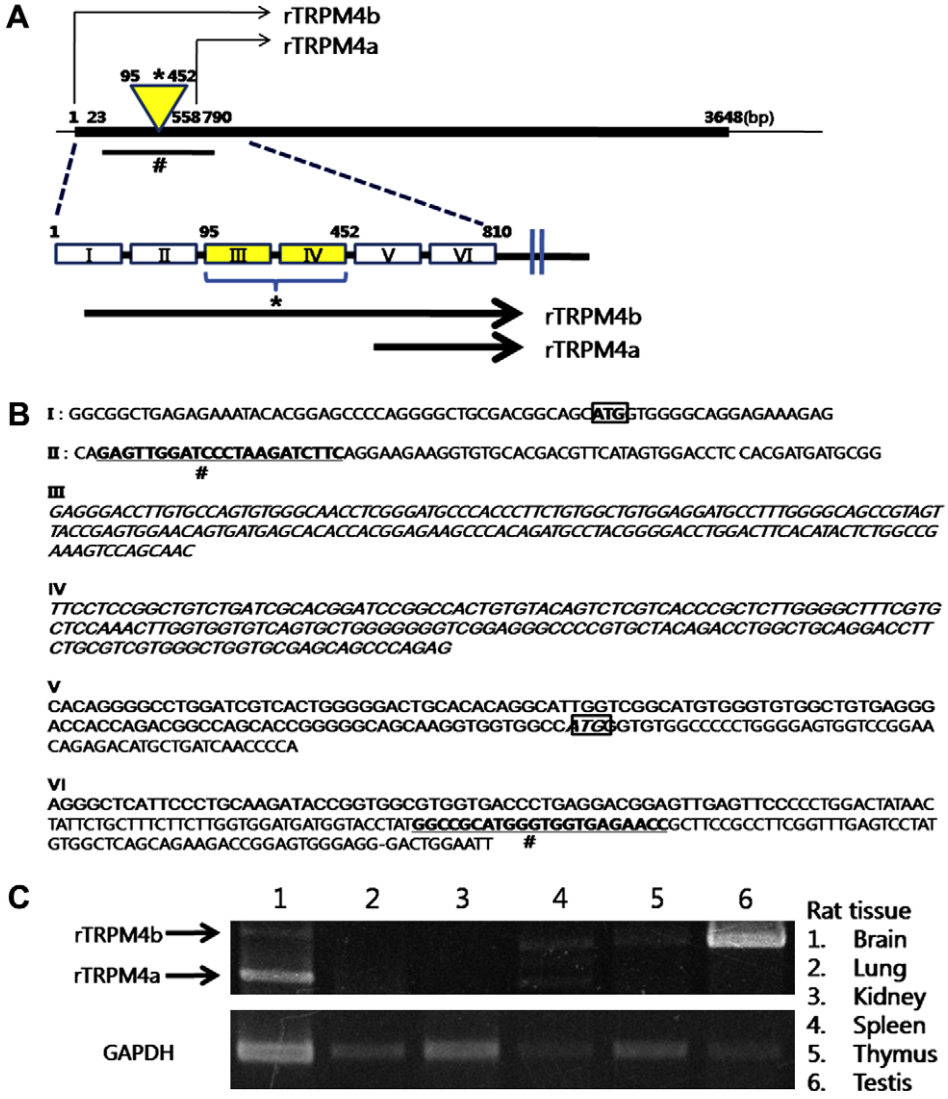

Fig. 2. Representation of coding start sites and deleted exons (A) and nucleotide sequence adjacent to the start codon of rTRPM4 isoforms (B). *Exons not contained in rTRPM4a. #Primers used to distinguish rTRPM4a and rTRPM4b. Sequences of exons III and IV, not contained in rTRPM4a, are in *italic* letters. Start codons for rTRPM4b and rTRPM4a are boxed. (C) Expression analysis of rTRPM4b (767-bp band) and rTRPM4a (410-bp band) by RT-PCR. Amplification of GAPDH was used as an internal control.

moderate expression in the brain, spleen, and thymus (Fig. 2C). In addition, rTRPM4a was expressed only in brain and spleen.

Subcellular localization and channel function of rTRPM4 isoforms

Subcellular localization of the rTRPM4 isoforms was examined by visualizing cells co-transfected with the GFP-TRPM4 isoforms and MN-DsRed DNA, a membrane staining marker (Fig. 3A and B). rTRPM4b was integrated into the endoplasmic reticulum (ER)/Golgi complex, some vesicle, and the plasma membrane. However, rTRPM4a was mainly integrated into the ER/Golgi complex and was rarely found in the plasma membrane. Furthermore, the both rTRPM4 proteins fused with GFP on their C-terminal displayed a similar cell expression pattern (data not shown). These data suggest that the N-terminal region of TRPM4b has a pivotal role in its cellular localization.

To further analyze the two rTRPM4 isoforms, we performed patch-clamp recordings. In the presence of 30 μM $[Ca^{2+}]_i$, whole-cell currents in rTRPM4b-overexpressing cells showed an outwardly rectifying I–V relationship (Fig. 3C). This finding is also a characteristic feature of human and mouse TRPM4b-mediated currents [10–12]. However, whole-cell currents in rTRPM4a-overexpressing cells were not different from those in non-transfected cells (Fig. 3C). This suggests that rTRPM4a is a non-functional channel similar to hTRPM4a [13].

Elevation of $[Ca^{2+}]_i$ resulted in a dose-dependent increase in rTRPM4b channel activity (Fig. 3D). Fitting the data plots with the dose–response logistic function revealed the EC_{50} value to be 1.12 ± 0.09 mM at −100 mV and 78 ± 11 μM at 100 mV, suggesting the voltage-dependent Ca^{2+} binding affinity of rTRPM4b (Fig. 3D). More than 10-fold higher Ca^{2+} levels are required for half maximal activation of rTRPM4b at −100 mV as compared to that at 100 mV (Fig. 3D). At 100 mV, the EC_{50} value for rTRPM4b is less than 100 μM, which is similar to that of hTRPM4b [10]. It is noteworthy that elevation of $[Ca^{2+}]_i$ led to an increase in P_o for rTRPM4b at negative potentials and at high Ca^{2+} levels. The P_o values for rTRPM4b were very similar at negative and positive potentials. This is in contrast to hTRPM4b, for which P_o is increased at positive potentials, but is almost unchanged at negative potentials [14]. TRPM4 channels with similar Ca^{2+} sensitivities were described in CHO cells [8] and rat brain capillary endothelium [15]. These results suggest that increasing $[Ca^{2+}]_i$ reduce voltage-dependence of the rTRPM4b channel activity, but not that of the hTRPM4b channel.

Comparison of the amino acid sequences and channel activity of rTRPM4b with those of hTRPM4b

Supplemental Fig. 1 depicts the corresponding amino acids of hTRPM4b with rTRPM4b. Alignments were performed using BLASTP. hTRPM4b and rTRPM4b had 81% (981/1198) identity and 88% (1058/1198) positives (http://www.ncbi.nlm.nih.gov/). hTRPM4b integrated into the ER/Golgi complex and plasma membrane in a similar fashion to rTRPM4b (Fig. 4A).

In inside-out patches, the rat or human TRPM4b channels were not observed in $[Ca^{2+}]_i$-free solutions (Fig. 4B). This shows that an rTRPM4b is Ca^{2+} activated channel as like hTRPM4b. rTRPM4b had a linear single-channel I–V relationship with a slope conductance of 16.11 ± 0.28 pS, while hTRPM4b had a single-channel slope

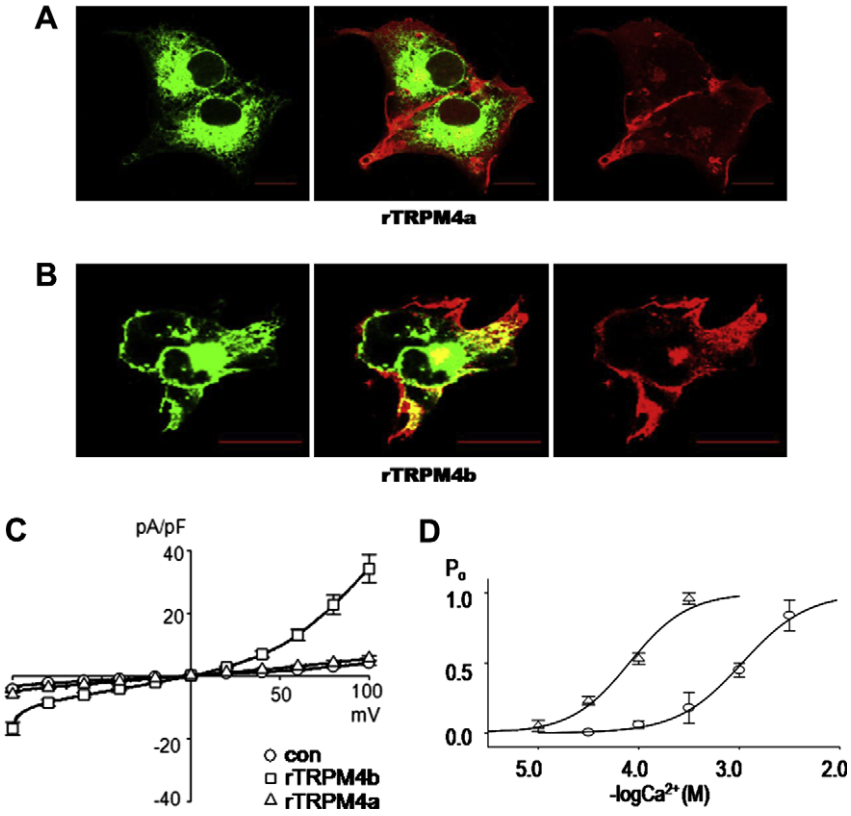

Fig. 3. Cellular localization of rTRPM4 isoforms. rTRPM4a (A) and rTRPM4b (B) were N-terminally fused to GFP and transiently expressed in COS-7 cells. Cells were also co-transfected with MN-DsRed, a plasma membrane marker. Intracellular localization of rTRPM4a and rTRPM4b were visualized by confocal microscopy (left panel). MN-DsRed, a membrane marker, indicated the plasma membrane of the cells (right panel). Co-localized regions are shown in yellow in the merged images (middle panel). Scale bars represent 20 μm. (C) Whole-cell currents of non-transfected HEK293T cells (*circles*; $n = 7$), cells transfected with rTRPM4b (*squares*; $n = 10$), and cells transfected with rTRPM4a (*triangles*; $n = 10$). Currents were activated by 30 μM $[Ca^{2+}]_i$. (D) Dose–response curve for Ca^{2+}-sensitivity of rTRPM4b. Circles represent dose responses at −100 mV, triangles represent dose responses at 100 mV. Data represent the mean ± SE of three to four channels ($P < 0.05$). Solid lines represent logistic function fittings.

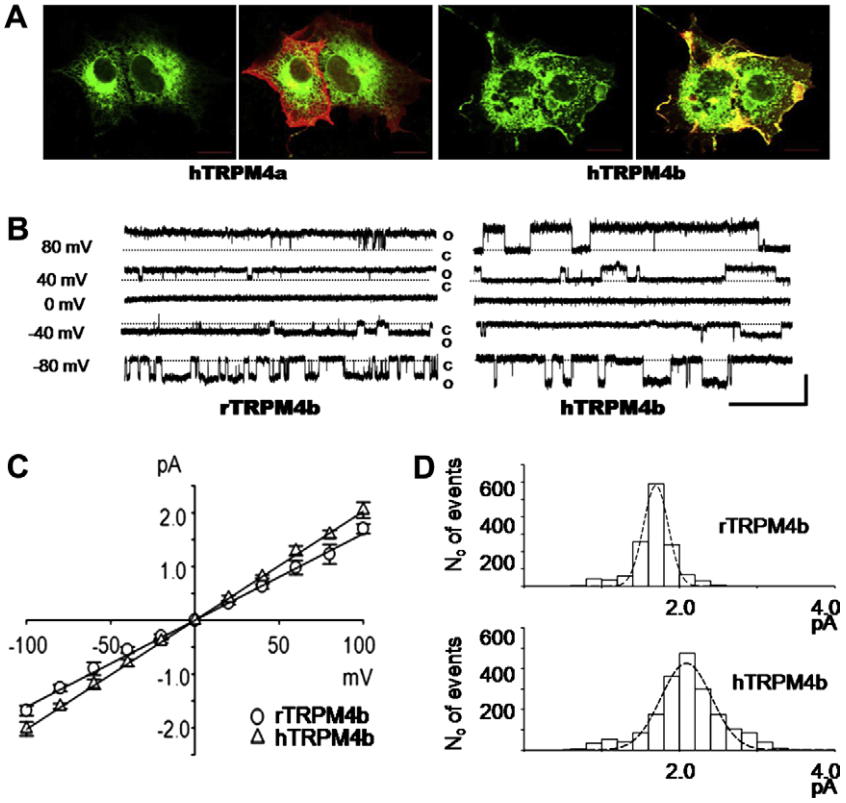

Fig. 4. (A) Subcellular localization of hTRPM4a and hTRPM4b. Both isoforms were N-terminally fused to GFP and transiently expressed in COS-7 cells. Intracellular localization of hTRPM4a and hTRPM4b in COS-7 cells were visualized by confocal microscopy. To delineate the plasma membrane, MN-DsRed, a membrane marker, was co-transfected with the channel constructs. Co-localized regions are shown in yellow in the merged images. Scale bars represent 20 μm. (B) Representative traces of rTRPM4b (left) and hTRPM4b (right) currents at different potentials in inside-out patches. Bars are scaled as 2 pA and 200 ms. (C) Single-channel I–V analysis of rTRPM4b and hTRPM4b. Current amplitudes of 5–9 channels were measured. rTRPM4b and hTRPM4b were activated by 300 μM and 1 μM $[Ca^{2+}]_i$, respectively. Data represent the mean ± SE, $P < 0.05$. (D) Representative histograms of single-channel current amplitudes of rTRPM4b and hTRPM4b channels.

conductance of 19.96 ± 0.02 pS when overexpressed in HEK293T cells (Fig. 4C and 4D). Thus, rTRPM4b has a lower single-channel conductance than does hTRPM4b. These results indicate that TRPM4b has, in general, similar channel features regardless of species, but that the channel conductance of TRPM4b does vary slightly between species.

Discussion

Here, we identified novel rTRPM4a and rTRPM4b. Comparison of the rTRPM4b amino acid sequence with hTRPM4b sequences revealed that TRPM4b is highly conserved. The results from the calcium-treatment experiments suggested that rTRPM4b is a calcium-activated cation channel, while rTRPM4a, the splice variant, is non-functional. Both human and rat GFP-TRPM4b were localized to the ER, Golgi, some vesicles, and the plasma membrane. However, rTRPM4a was rarely localized to the plasma membrane during fluorescence imaging experiments. Therefore, since rTRPM4a lacks the N-terminus, the N-terminal region of rTRPM4b likely plays a key role in both its cellular localization and its functionality.

The putative rTRPM4b sequence derived from the rat genomic project supports our 5′-RACE–PCR sequence data. It was previously reported that hTRPM4a in T cells suppressed active hTRPM4b currents by influencing receptor-mediated Ca^{2+} mobilization [13]. Furthermore, mutation of the hTRPM4 N-terminus impaired endocytosis and led to an elevated hTRPM4 channel density at the cell surface [9]. Based on previous reports and the data presented here, we are further examining the role of the N-terminal region of TRPM4b.

This paper reports the genetic organization of the rTRPM4 gene. The full-length gene, consisting of exons I–V, was termed rTRPM4b. An alternative splicing isoform which lacks exons III and IV has been termed rTRPM4a. The initiation codon for rTRPM4a is in exon V. Tissue distribution analyses revealed that rTRPM4b was expressed at high levels in testis. This suggests that active rTRPM4b may be more highly expressed in actively dividing tissues. A third splicing variant of rTRPM4 was cloned (data not shown) and is currently being further examined.

Human and mouse TRPM4b are Ca^{2+}-activated non-selective cation channels [3]. We confirmed that rTRPM4b is also a Ca^{2+}-activated channel (Fig. 3D). Furthermore, increasing $[Ca^{2+}]_i$ reduced the voltage-dependence of rTRPM4b channel activity, but not that of hTRPM4b (Fig. 3D) [10]. This finding is very interesting because the same TRPM4 channel in humans and rats has different channel regulation. Though comparative channel studies between species are rare, it is necessary to gain a more complete understanding of TRPM4. Cellular localization and channel activities were very similar between human and rat TRPM4b. It would be interesting to study the binding proteins and transport regulation mechanisms that the TRPM4 channel uses to translocate from the ER/Golgi complex to the plasma membrane.hTRPM4b and rTRPM4b have an 81% amino acid homology, similar localization pattern, and parallel single-channel I–V curves. However, these channels do display slightly different open probabilities and conductance. This may be due to differences of the amino acid sequence within the intracellular domain. It would be interesting to identify the regulatory amino acid sequence of TRPM4 or other channel proteins that have varying conductance between species.

In conclusion, we identified rTRPMb and rTRPM4a channels, which are orthologues of hTRPM4b and hTRPM4a. These isoforms vary in their tissue and cellular distribution, as well as in their functionality. Furthermore, we measured the channel current and Ca^{2+} dependency of rTRPM4b, which differed from hTRPM4b. It is very interesting discovery that same channels have different Ca^{2+} dependency along with species.

Acknowledgement

This work was supported by the Basic Research Program of the Korea Science & Engineering Foundation (R13-2005-012-02002-0) and a National Research Foundation of Korea Grant (2009-0067148). J.C.Y., E.K., D.K., and N.P. were supported by the Brain Korea 21 Programs.

Appendix A. Supplementary data

Supplementary data associated with this article can be found, in the online version, at doi:10.1016/j.bbrc.2009.11.142.

References

[1] C. Montell, G.M. Rubin, Molecular characterization of the Drosophila trp locus: a putative integral membrane protein required for phototransduction, Neuron 2 (1989) 1313–1323.
[2] X.Z. Xu, F. Moebius, D.L. Gill, C. Montell, Regulation of melastatin, a TRP-related protein, through interaction with a cytoplasmic isoform, Proc. Natl. Acad. Sci. USA 98 (2001) 10692–10697.
[3] P. Launay, A. Fleig, A.L. Perraud, A.M. Scharenberg, R. Penner, J.P. Kinet, TRP4M is a Ca2þ-activated nonselective cation channel mediating cell membrane depolarization, Cell 109 (2002) 397–407.
[4] C. Harteneck, Function and pharmacology of TRPM cation channels, Naunyn-Schmiedeberg's Arch. Pharmacol. 371 (2005) 307–314.
[5] G. Owsianik, K. Talavera, T. Voets, B. Nilius, Permeation and selectivity of TRP channels, Annu. Rev. Physiol. 68 (2006) 685–717.
[6] M. Murakami, F. Xu, I. Miyoshi, E. Sato, K. Ono, T. Iijima, Identification and characterization of the murine TRPM4 channel, Biochem. Biophys. Res. Commun. 307 (2003) 522–528.
[7] J.Y. Park, E.M. Hwang, O. Yarishkin, J.H. Seo, E. Kim, J. Yoo, G.M. Yi, D.G. Kim, N. Park, C.M. Ha, J.H. La, D. Kang, J. Han, U. Oh, S.G. Hong, TRPM4b channel suppresses store-operated Ca^{2+} entry by a novel protein–protein interaction with the TRPC3 channel, Biochem. Biophys. Res. Commun. 368 (2008) 677–683.
[8] O.V. Yarishkin, E.M. Hwang, J.H. Park, D. Kang, J. Han, S.G. Hong, Endogenous TRPM4-like channel in Chinese hamster ovary (CHO) cells, Biochem. Biophys. Res. Commun. 369 (2008) 712–717.
[9] M. Kruse, E. Schulze-Bahr, V. Corfield, A. Beckmann, B. Stallmeyer, G. Kurtbay, I. Ohmert, E. Schulze-Bahr, P. Brink, O. Pongs, Impaired endocytosis of the ion channel TRPM4 is associated with human progressive familial heart block type I, J. Clin. Invest. 119 (2009) 2737–2744.
[10] R. Vennekens, B. Nilius, Insights into TRPM4 function, regulation and physiological role, Handb. Exp. Pharmacol. 179 (2007) 269–285.
[11] P. Launay, A. Fleig, A.L. Perraud, A.M. Scharenberg, R. Penner, J.P. Kinet, TRPM4 is a Ca^{2+}-activated nonselective cation channel mediating cell membrane depolarization, Cell 109 (2002) 397–407.
[12] N.D. Ullrich, T. Voets, J. Prenen, R. Vennekens, K. Talavera, G. Droogmans, B. Nilius, Comparison of functional properties of the Ca^{2+}-activated cation channel TRPM4 and TRPM5 from mice, Cell. Calcium 37 (2005) 267–278.
[13] P. Launay, H. Cheng, S. Srivatsan, R. Penner, A. Fleig, J.P. Kinet, TRPM4 regulates calcium oscillations after T cell activation, Science 306 (2004) 1374–1377.
[14] B. Nilius, J. Prenen, A. Janssens, T. Voets, G. Droogmans, Decavanadate modulates gating of TRPM4 cation channels, J. Physiol. 560 (2004) 753–765.
[15] L. Csanády, V. Adam-Vizi, Ca^{2+}- and voltage-dependent gating of Ca^{2+}- and ATP-sensitive cationic channels in brain capillary endothelium, Biophys. J. 85 (2003) 313–327.